

Trapping N₂ and CO₂ on the Sub-Nano Scale in the Confined Internal Spaces of Open-Cage C₆₀ Derivatives: Isolation and Structural Characterization of the Host–Guest Complexes

Tsukasa Futagoishi, Michihisa Murata, Atsushi Wakamiya, and Yasujiro Murata*

Abstract: An open-cage C₆₀ tetraketone with a large opening was able to encapsulate N₂ and CO₂ molecules after its exposure to high pressures of N₂ and CO₂ gas. A subsequent selective reduction of one of the four carbonyl groups on the rim of the opening induced a contraction of the opening (→**2**) and trapped the guest molecules inside **2**. The thus-obtained host–guest complexes N₂@**2** and CO₂@**2** could be isolated by recycling HPLC, and were found to be stable at room temperature. The molecular structures of N₂@**2** and CO₂@**2** were determined by single-crystal X-ray diffraction analyses, and revealed a short N≡N triple bond for the encapsulated N₂, as well as an unsymmetric molecular structure for the encapsulated molecule of CO₂. The IR spectrum of CO₂@**2** suggested that the rotation of the encapsulated molecule of CO₂ is partially restricted, which was supported by DFT calculations.

Small and structurally simple gaseous molecules such as N₂ and CO₂ are ubiquitous in the atmosphere. The fundamental properties and structures of these molecules have been extensively investigated by spectroscopic methods, both in the gas phase and in the solid state, for example, by Raman^[1] and IR spectroscopy,^[2] electron diffraction,^[3] as well as powder X-ray diffraction analysis under high-pressure conditions (e.g. 28 GPa at 680 K).^[4] If these molecules can be selectively trapped in a suitable confined space, studies on the intrinsic properties of the guest molecules and the interactions between host and guest molecules, as well as the dynamic behavior of the guest molecules should become attainable. In addition, these studies can be conducted both in solution and in the solid state at ambient temperature and pressure. Although micro-porous materials with suitable pore sizes and many kinds of clathrates are commonly used for the separation and storage of such gaseous molecules,^[5] it is still difficult to keep a single gaseous molecule in a distinct molecular container under ambient conditions. The design and development of such molecular containers with a discrete structure for the uptake of gaseous molecules thus represent attractive research targets.

Open-cage fullerenes exhibit specific and rigid structures based on bowl-shaped skeletons.^[6] If their openings are sufficiently large enough for the targeted molecules to be encapsulated, the guest molecules can be accommodated in the confined space on the sub-nano scale within these open-cage fullerene derivatives. The formation of corresponding 1:1 host-guest complexes, consisting of an open-cage C₆₀ and a small molecule such as He,^[7] H₂,^[8] H₂O,^[9] NH₃,^[10] CH₄,^[11] CO,^[12] N₂,^[13] or HF,^[14] has been reported previously. Based on the van der Waals radii of these elements (C = 1.70 Å; N = 1.60 Å; O = 1.50 Å)^[15] in the encapsulated species, the length of the major and minor axes of N₂ can be estimated as 4.3 and 3.2 Å, respectively. There is no report on the encapsulation of CO₂, with the axes of 5.3 and 3.4 Å, as the size requirements of CO₂ exceed the internal space of pristine C₆₀ with a diameter of 3.7 Å.

Accordingly, it should be of great interest to study the encapsulation of CO₂ in suitable open-cage C₆₀ derivatives, and to investigate their dynamic behavior, both with regard to the size of the opening and the internal space. However, in many cases the encapsulated species easily escape from the open-cage fullerenes.^[10,14] Such an escape should become less likely, if either stable molecular complexes arise from attractive interactions and/or the opening is contracted chemically.^[16] Herein, we report 1) the encapsulation of N₂ and CO₂ within an open-cage C₆₀, 2) the molecular structures of these host–guest complexes, obtained from single-crystal X-ray diffraction analyses, and 3) the rotational and vibrational behavior of the encapsulated molecule.

We have reported the synthesis of open-cage C₆₀ **1** with a circular 17-membered-ring opening, which contains one sulfur atom on the rim.^[17] The theoretically calculated structure of **1**,^[18] in which the *tert*-butyl groups were replaced by hydrogen atoms, suggested an elliptical shape for the opening (Figure 1). Based on the ¹H NMR spectroscopic analysis at room temperature, the rapid in/out exchange of water indicated that the opening of **1** is larger than that of the compound prepared by Iwamatsu et al.,^[19] demonstrating that **1** may serve as a new molecular host for various small molecules. To prevent a facile escape, as described above, we envisioned, based on the previous work, that an effective strategy could be the introduction of a stopper on the opening.^[16] A selective reaction of one of the four carbonyl groups on the rim of open-cage C₆₀ **1** with a hydride source would afford alcohol (giving cage **2**), in which the OH moiety should be able to act as such a stopper (Figure 1).

However, DFT calculations at the M06-2X/6-31G* level of theory did not support our hypothesis of a selective formation of alcohol **2**. Nevertheless, the reaction of tetrake-

[*] T. Futagoishi, Dr. M. Murata, Prof. Dr. A. Wakamiya, Prof. Dr. Y. Murata
Institute for Chemical Research
Kyoto University
Uji, Kyoto 611-0011 (Japan)
E-mail: yasujiro@scl.kyoto-u.ac.jp

Supporting information for this article is available on the WWW under <http://dx.doi.org/10.1002/anie.201507785>.

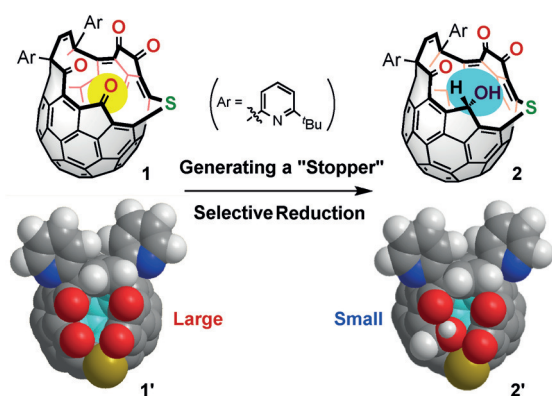
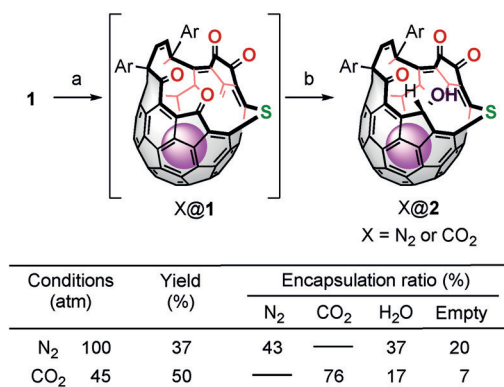


Figure 1. Structural formula of **1** and **2**, as well as top views (space-filling models) of the corresponding optimized structures of **1'** and **2'**, in which *tert*-butyl groups were replaced with hydrogen atoms; calculated at the M06-2X/6-31C* level of theory. C gray, O red, H white, S gold, N dark blue, inside of the cavity light blue.

tone **1** with NaBH₄ in a mixture of *o*-dichlorobenzene (ODCB) and EtOH at 0°C afforded alcohol **2** isolated in 47% yield. The structure of **2** was determined by single crystal X-ray diffraction analysis (see below). Thus, this reaction can be used to install a stopper on the rim of **1** after the encapsulation of a guest. According to DFT calculations, the required energies for insertion of N₂ and CO₂ into tetraketone **1'** should be expected to be 8.5 and 4.3 kcal mol⁻¹, respectively. These results suggested a facile encapsulation of both N₂ and CO₂ at room temperature. Upon formation of alcohol **2'**, these values increased to 22.2 and 12.3 kcal mol⁻¹, respectively, reflecting the contraction of the opening relative to **1'**.

After having obtained these values, insertion of N₂ into **1** was attempted. A powdered sample of H₂O@**1** was heated to 140°C under vacuum for 14 h, to remove the encapsulated water molecule. Subsequently, **1** was subjected to 100 atm of N₂ gas at room temperature for 24 h. Then, the resulting powder was dissolved in ODCB at 0°C, and treated with NaBH₄ in EtOH (Scheme 1). This reaction has to be quenched after a short reaction time (15 min) to avoid reduction of more than one carbonyl group. Alcohol **2** was obtained in 37% yield and proved to be a mixture of N₂@**2**,



Scheme 1. Synthesis of N₂@**2** and CO₂@**2** from **1**. Reagents and conditions: a) N₂ (100 atm) or CO₂ (45 atm), RT, 24 h; b) NaBH₄ (0.5 equiv, 15 mm in EtOH), ODCB, 0°C, 15 min, then quenched with NH₄Cl aq.

H₂O@**2**, and empty **2**. The N₂ encapsulation ratio was determined by integration of the new OH signals in the ¹H NMR spectrum for N₂@**2** (43%). It is assumed that H₂O@**2** was formed during the work-up process.

Despite the molecular size of CO₂, an encapsulation of CO₂ within **1** was also achieved under similar conditions, that is, treatment of **1** with 45 atm of CO₂ gas, followed by reduction with NaBH₄ resulted in the formation of CO₂@**2** in 50% yield with a 76% CO₂ encapsulation ratio. The molecular host–guest complex CO₂@**2** is, to our knowledge, the first example of an open-cage fullerene derivative encapsulating a CO₂ molecule. In the absence of a stopper, that is, in CO₂@**1**, the CO₂ encapsulation ratio decreased from 72% to 46% after 100 h at room temperature. Owing to the contraction of the opening in **2**, in addition to the stabilization energies of 16.7 and 20.0 kcal mol⁻¹ for N₂@**2'** and CO₂@**2'**, respectively, the encapsulated N₂ and CO₂ were fully maintained inside **2** for 100 h at room temperature. The CO₂ did not escape from CO₂@**2** after heating at 50°C for 37 h, while only 5% escape was observed after heating at 100°C for 63 h. Thus, the stopper in **2** is able to effectively prevent the release of the encapsulated N₂ and CO₂.

After the formation of N₂@**2** and CO₂@**2**, the separation of these molecular complexes from H₂O@**2** and empty **2** was achieved by recycling HPLC with Cosmosil Buckyprep columns. In the case of a mixture of N₂@**2**, H₂O@**2**, and empty **2**, a complete separation into two HPLC peaks was accomplished after the 15th cycle (Figure S10). From the first fraction, a mixture of H₂O@**2** and empty **2** was obtained. The ¹H NMR spectrum measured in CDCl₃ exhibited a sharp signal corresponding to the encapsulated water at δ = −11.07 ppm and suggested an encapsulation ratio of around 76%. For H₂O@**1** (that is, without the stopper), in contrast, a broad signal at δ = −11.48 ppm was observed.^[17] This difference reflects the stopper-induced suppression of in/out exchange of the water.^[19] From the second fraction, pure N₂@**2** was isolated. Molecular complex CO₂@**2** was also isolated in a similar fashion. Interestingly, in the case of CO₂@**2**, a complete peak separation was achieved after just the 3rd cycle (Figure S11). This result indicated that CO₂@**2** is subjected to a significantly higher degree of van der Waals interactions between the molecular complex and the stationary materials of the HPLC relative to N₂@**2**, H₂O@**2**, and empty **2**. These interactions should most likely be affected by the interaction between the fullerene and the entrapped guest.

The ¹H NMR signals of open-cage C₆₀ **2** in CD₂Cl₂ were observed to shift upon encapsulation of the guests.^[12,13] For example, the signals corresponding to the methine proton, which are spatially in close proximity to the encapsulated guests, were observed at δ = 7.50, 7.44, 7.42, and 7.41 ppm for CO₂@**2**, N₂@**2**, H₂O@**2**, and empty **2**, respectively. Although the *tert*-butyl protons on the pyridyl moieties are located far away from the guests, they were also subjected to such signal shifts. This result implied that the weak interaction caused by the encapsulation is distributed over the whole host molecule, most likely due to small structural changes on the C₆₀ cage. The ¹³C NMR spectrum of CO₂@**2** in CDCl₃ showed a signal for the encapsulated CO₂ at δ = 112.83 ppm, which is

12.16 ppm upfield shifted relative to free CO₂ ($\delta = 124.99$ ppm),^[20] reflecting the strong shielding effect of the fullerene cage.

One advantage of using open-cage C₆₀ **2** as a host is its high tendency to crystallize from benzene solutions in the presence of nickel(II) octaethylporphyrin, and single crystals of CO₂@**2**, N₂@**2**, and H₂O@**2** were obtained in such a fashion. X-ray diffraction data were collected at -170 or -173 °C, and allowed an unambiguous determination of the molecular structures (Figure 2a–c). The structural analyses revealed that CO₂, N₂, and H₂O are located at the center of the fullerene cage with occupancies of 0.916(4), 0.995(5), and 0.906(7), respectively, representing encapsulation ratios of 92% (CO₂), 100% (N₂), and 91% (H₂O). The slightly diminished value for CO₂ should be ascribed to an escape of CO₂ during crystallization, while the higher value for H₂O relative to that in solution (ca. 76%) should be assigned to an enrichment in the crystals.^[9b,c,17] In agreement with the results from DFT calculations, the size of the opening in **2** is substantially smaller than that of **1**, that is, values of 6.878(2) and 3.033(3) Å were measured for the long S(1)–C(11) and the short O(1)–C(6) axes in H₂O@**2** (Figure 2d), whereas the corresponding values in H₂O@**1** are 6.804(3) and 4.323-

(4) Å.^[17] These results confirmed the contraction of the opening in open-cage C₆₀ **2**.

The encapsulated CO₂ and N₂ were found to be compressed in size compared to free CO₂ and N₂. A bond length of 1.032(3) Å was observed for the N≡N triple bond in **2**, which corresponds to a 5.7% decrease relative to that of free N₂ in the gas phase (1.094 Å).^[21] Such compression of encapsulated CO was also observed for the Gan's compounds, in which several short contacts were observed between the encapsulated CO and the fullerene cage.^[12b] Although no apparent short contact between the N₂ and the fullerene cage was observed, small interaction between them detected by ¹H NMR and HPLC analyses might induce this shortening. Of particular interest is the unsymmetric shape of the encapsulated CO₂ (Figure 2a). The C=O(6) bond (1.105(4) Å) was slightly shorter than the C=O(5) bond (1.166(4) Å), and the latter is almost the length of the symmetrical bonds observed for CO₂ in the gas phase (1.1602(8) Å).^[3] This shortening of one of the C=O bonds was also reported for CO₂ trapped in metal–organic frameworks (MOFs).^[22] In addition, we observed 24 contacts (O_{CO2}...C_{openC60} 3.02–3.21 Å and C_{CO2}...C_{openC60} 3.35–3.39 Å) that are shorter than the sum of the van der Waals radii (O...C: 3.22 Å; C...C: 3.40 Å), reflecting strong interactions between the CO₂ and **2** (Figure S16). These results are in good agreement with the observed differences in the HPLC analysis and the ¹H NMR measurements between CO₂@**2** and N₂@**2**.

Molecular complexes CO₂@**2** and N₂@**2** should thus allow studies on the intrinsic properties of confined CO₂ and N₂ in sub-nano scale spaces. Unfortunately, the Raman band of the encapsulated N₂ was not detected clearly, owing to the weak intensity of its stretching band, which is consistent with results from DFT calculations (Figure S12). In contrast, the IR spectrum of CO₂@**2** exhibited a sharp band for the CO₂ at 2334 cm⁻¹, corresponding to the antisymmetric stretch (Figure 3). Usually, the IR spectra of gaseous CO₂ show two broad bands at 2342 and 2361 cm⁻¹,^[2] which arise from the rotation of CO₂ (Figure 3b). The presence of only one absorption band in the IR spectrum of CO₂@**2** suggested that the rotational freedom of the CO₂ is restricted, probably due to constraints by the internal space.^[12,23] To obtain further insight regarding the rotational behavior of the CO₂ encapsulated in **2**, DFT calculations were carried out at the M06-2X/3-21G level of theory. The rotation of the CO₂ may be described as the dynamic exchange motion between the upper oxygen atom and the lower one in the optimized structures. For such a process, we found a transition state, which was 8.1 kcal mol⁻¹ higher in energy relative to the most stable conformation. This result suggested that a rotation of the CO₂ should be possible at room temperature, and that the suppression of the rotation might be due to the shape of both the opening and the internal space.

In conclusion, the molecular host–guest complexes N₂@**2** and CO₂@**2** were obtained by incorporating gaseous N₂ and CO₂ into open-cage C₆₀**1**, followed by installation of a hydroxy stopper at the rim of the opening. Isolation of pure N₂@**2** and CO₂@**2** was accomplished by HPLC. Molecular complex CO₂@**2** is the first example for an open-cage C₆₀ encapsulating CO₂. The molecular structures of N₂@**2** and CO₂@**2** were

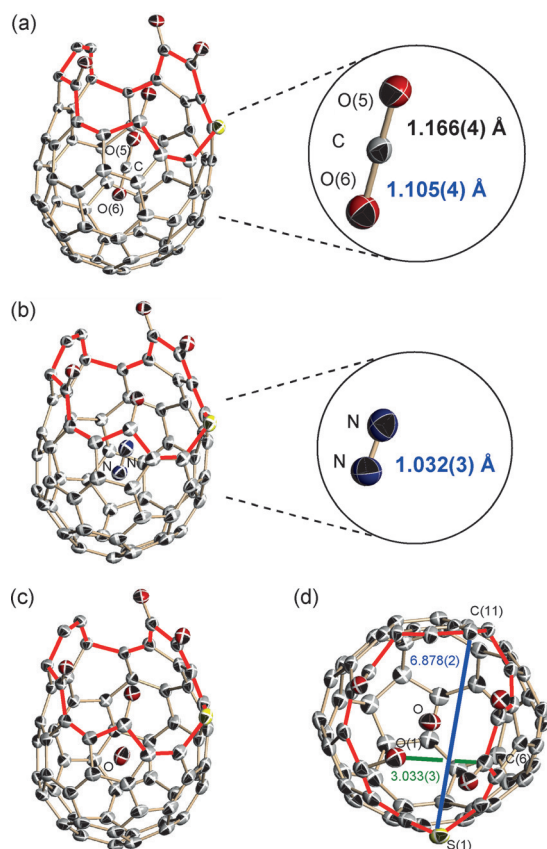


Figure 2. Single-crystal X-ray structures of a) CO₂@**2**, b) N₂@**2**, and c) H₂O@**2**. Encapsulated molecules are shown separately in the insets of (a) and (b). A top view of H₂O@**2** is shown in (d) to illustrate the size of the opening. Selected bond lengths are in [Å]. Thermal ellipsoids are set at 50% probability, while hydrogen atoms, solvent molecules, *tert*-butylpyridyl groups, and nickel(II) octaethylporphyrin are omitted for clarity. Red line marks the edge of the opening. The blue line is the long axis, the green line is the short axis.

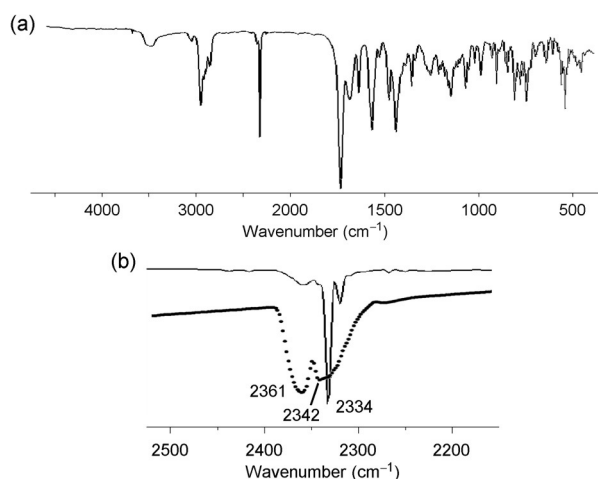


Figure 3. IR spectrum (KBr) of a) $\text{CO}_2@2$ and b) expanded superposition of IR spectra of $\text{CO}_2@2$ (solid line) and gaseous CO_2 (dotted line) for comparison.

clearly determined by single-crystal X-ray diffraction analyses, revealing a contracted $\text{N}\equiv\text{N}$ triple bond for the N_2 relative to free N_2 in the gas phase, as well as an unsymmetric shape of the CO_2 . IR spectroscopy measurements showed that the rotational behavior of the encapsulated CO_2 is partially restricted, which was supported by DFT calculations. Encapsulation of other small molecules is currently ongoing in our laboratory.

Acknowledgements

We would like to thank Dr. Takehiro Ohta and Prof. Dr. Takashi Ogura at the Picobiology Institute, Graduate School of Life Science, University of Hyogo, for their support with the Raman measurements. Financial support was partially provided by the PRESTO program on “Molecular Technology and Creation of New Functions” from the JST and the JSPS KAKENHI (grant no. 23241032, 15H00993, 15H00939, and 15K13641). The NMR measurements were supported by the Joint Usage/Research Center (JURC) at the ICR, Kyoto University. Parts of the X-ray measurements were carried out at the SPring-8 (BL38B1) with the approval of JASRI (2013A1489).

Keywords: CO_2 · fullerenes · host–guest chemistry · N_2 · open-cage C_{60}

How to cite: *Angew. Chem. Int. Ed.* **2015**, *54*, 14791–14794
Angew. Chem. **2015**, *127*, 15004–15007

- [1] a) D. Schiferl, S. Buchsbaum, R. L. Mills, *J. Phys. Chem.* **1985**, *89*, 2324–2330; b) H. Olijnyk, A. P. Jephcoat, *Phys. Rev. B* **1998**, *57*, 879–888.
- [2] a) S. Bauerecker, F. Taucher, C. Weitkamp, W. Michaelis, H. K. Cammenga, *J. Mol. Struct.* **1995**, *348*, 237–242; b) R. Kumar, S. Lang, P. Englezos, J. Ripmeester, *J. Phys. Chem. A* **2009**, *113*, 6308–6313; c) D. Serra, M. C. Correia, L. McElwee-White, *Organometallics* **2011**, *30*, 5568–5577.

- [3] A. G. Gershiikov, V. P. Spiridonov, *J. Mol. Struct.* **1982**, *96*, 141–149.
- [4] C. S. Yoo, H. Kohlmann, H. Cynn, M. F. Nicol, V. Iota, T. LeBihan, *Phys. Rev. B* **2002**, *65*, 104103.
- [5] a) M. Pera-Titus, *Chem. Rev.* **2014**, *114*, 1413–1492; b) S. Horike, S. Shimomura, S. Kitagawa, *Nat. Chem.* **2009**, *1*, 695–704; c) E. D. Sloan, *Nature* **2003**, *426*, 353–359; d) J. J. Gassensmith, H. Furukawa, R. A. Smaldone, R. S. Forgan, Y. Y. Botros, O. M. Yaghi, J. F. Stoddart, *J. Am. Chem. Soc.* **2011**, *133*, 15312–15315; e) H. Tsue, K. Matsui, K. Ishibashi, H. Takahashi, S. Tokita, K. Ono, R. Tamura, *J. Org. Chem.* **2008**, *73*, 7748–7755.
- [6] G. C. Vougioukalakis, M. M. Roubelakis, M. Orfanopoulos, *Chem. Soc. Rev.* **2010**, *39*, 817–844.
- [7] a) Y. Rubin, T. Jarroson, G.-W. Wang, M. D. Bartberger, K. N. Houk, G. Schick, M. Saunders, R. J. Cross, *Angew. Chem. Int. Ed.* **2001**, *40*, 1543–1546; *Angew. Chem.* **2001**, *113*, 1591–1594; b) C. M. Stanisky, R. J. Cross, M. Saunders, M. Murata, Y. Murata, K. Komatsu, *J. Am. Chem. Soc.* **2005**, *127*, 299–302; c) Y. Morinaka, F. Tanabe, M. Murata, Y. Murata, K. Komatsu, *Chem. Commun.* **2010**, *46*, 4532–4534.
- [8] Y. Murata, M. Murata, K. Komatsu, *J. Am. Chem. Soc.* **2003**, *125*, 7152–7153.
- [9] a) S.-i. Iwamatsu, T. Uozaki, K. Kobayashi, S. Re, S. Nagase, S. Murata, *J. Am. Chem. Soc.* **2004**, *126*, 2668–2669; b) Z. Xiao, J. Yao, D. Yang, F. Wang, S. Huang, L. Gan, Z. Jia, Z. Jiang, X. Yang, B. Zheng, G. Yuan, S. Zhang, Z. Wang, *J. Am. Chem. Soc.* **2007**, *129*, 16149–16162; c) S. Liu, Q. Zhang, Y. Yu, L. Gan, *Org. Lett.* **2012**, *14*, 4002–4005.
- [10] K. E. Whitener, Jr., M. Frunzi, S.-i. Iwamatsu, S. Murata, R. J. Cross, M. Saunders, *J. Am. Chem. Soc.* **2008**, *130*, 13996–13999.
- [11] K. E. Whitener, Jr., R. J. Cross, M. Saunders, S.-i. Iwamatsu, S. Murata, N. Mizorogi, S. Nagase, *J. Am. Chem. Soc.* **2009**, *131*, 6338–6339.
- [12] a) S.-i. Iwamatsu, C. M. Stanisky, R. J. Cross, M. Saunders, N. Mizorogi, S. Nagase, S. Murata, *Angew. Chem. Int. Ed.* **2006**, *45*, 5337–5340; *Angew. Chem.* **2006**, *118*, 5463–5466; b) L. Shi, D. Yang, F. Colombo, Y. Yu, W.-X. Zhang, L. Gan, *Chem. Eur. J.* **2013**, *19*, 16545–16549.
- [13] C. M. Stanisky, R. J. Cross, M. Saunders, *J. Am. Chem. Soc.* **2009**, *131*, 3392–3395.
- [14] A. Krachmalnicoff, R. Bounds, S. Mamone, M. H. Levitt, M. Carravetta, R. J. Whitby, *Chem. Commun.* **2015**, *51*, 4993–4996.
- [15] A. Bondi, *J. Phys. Chem.* **1964**, *68*, 441–451.
- [16] a) S.-C. Chuang, Y. Murata, M. Murata, K. Komatsu, *Chem. Commun.* **2007**, 1751–1753; b) Q. Zhang, T. Pankewitz, S. Liu, W. Klopper, L. Gan, *Angew. Chem. Int. Ed.* **2010**, *49*, 9935–9938; *Angew. Chem.* **2010**, *122*, 10131–10134.
- [17] T. Futagoishi, M. Murata, A. Wakamiya, T. Sasamori, Y. Murata, *Org. Lett.* **2013**, *15*, 2750–2753.
- [18] Gaussian 09 (Revision B.01), M. J. Frisch, et al., Gaussian, Inc.: Wallingford, CT, **2010**.
- [19] M. Frunzi, A. M. Baldwin, N. Shibata, S.-I. Iwamatsu, R. G. Lawler, N. J. Turro, *J. Phys. Chem. A* **2011**, *115*, 735–740.
- [20] G. R. Fulmer, A. J. M. Miller, N. H. Sherden, H. E. Gottlieb, A. Nudelman, B. M. Stoltz, J. E. Bercaw, K. I. Goldberg, *Organometallics* **2010**, *29*, 2176–2179.
- [21] J. Andzelm, E. Wimmer, *J. Chem. Phys.* **1992**, *96*, 1280–1303.
- [22] R. Vaidhyanathan, S. S. Iremonger, G. K. H. Shimizu, P. G. Boyd, S. Alavi, T. K. Woo, *Science* **2010**, *330*, 650–653.
- [23] S. Saint Martin, S. Marre, P. Guionneau, F. Cansell, J. Renouard, V. Marchetto, C. Aymonier, *Chem. Eur. J.* **2010**, *16*, 13473–13478.

Received: August 20, 2015

Published online: October 16, 2015